Asian Journal of Chemistry; Vol. 33, No. 5 (2021), 1144-1152

ASIAN JOURNAL OF CHEMISTRY

https://doi.org/10.14233/ajchem.2021.23162

Manganese(IV) Complexes Derived from Polyfunctional Dihydrazone: Structural, Electrochemical and Antimicrobial Studies

P. SARMA[1], P. MAHANTA[1], D. BASUMATARY[1,*] and C. MEDHI[2]

[1]Department of Applied Sciences, Gauhati University, Guwahati-781014, India
[2]Department of Chemistry, Gauhati University, Guwahati-781014, India

*Corresponding author: Tel: +91 361 2570412; E-mail: debbasumatary@gmail.com; debbasumatary@gauhati.ac.in

Received: 8 February 2021; *Accepted*: 20 March 2021; *Published online*: 16 April 2021; AJC-20337

Manganese(IV) complexes *viz.* $[Mn^{IV}(nagh)(A)_2]\cdot 2H_2O$ and $[Mn^{IV}(nagh)(NN)]$ have been synthesized from ligand *bis*(2-hydroxy-1-naphthaldehyde)glutaryldihydrazone ($naghH_4$) and auxiliary ligands, A = H_2O (**1**)/pyridine (**2**)/2-picoline (**3**)/3-picoline (**4**)/ 4-picoline (**5**) or NN = 2,2′-bipyridine (**6**)/1,10-phenanthroline (**7**). The elemental analysis, mass spectral and thermal studies supported the composition of all the manganese(IV) complexes. Structural aspects were determined from magnetic susceptibility, molar conductivity and spectral studies *i.e.* electronic, electron spin resonance and infrared. Their non-electrolytic nature were determined from molar conductances. Results from studies of magnetic moment, electronic and ESR suggested Mn(IV) ion in six-coordinate octahedral stereochemistry. The ligand coordinated to the metal in enolic form as a tetradentate in an *anti-cis* configuration as was correlated from IR data. Redox activities and antimicrobial potential against few Gram-positive and Gram-negative bacteria have been investigated for the dihydrazone and some manganese(IV) complexes.

Keywords: Manganese(IV), *bis*(2-Hydroxy-1-napthaldehyde)glutaryldihydrazone, Antimicrobial activity.

INTRODUCTION

Metal complexes derived from Schiff bases have been extensively studied and have played a crucial role in the progress of coordination chemistry. Having twin azomethine (-C=N-) and secondary amide (R-CO-NH-) functional groups, the dihydrazones form a significant class of the Schiff bases [1]. Dihydrazones that are obtained by condensation of *o*-hydroxy aromatic aldehydes and ketones with acylhydrazines, aroylhydrazines or pyridyl hydrazines contain additional phenol/naphthol groups, which further attribute to their potential as polynucleating ligands [2]. These ligands can react with metal ions either in *keto*, *enol* or *keto-enol* form to yield mononuclear or polynuclear complexes having discrete molecularity [2,3]. As reported by a few researchers [2,4,5], the electron-rich dihydrazones can stabilize the metal ions in its high oxidation states with diverse structural conformations. Additionally, different factors like the preparation method, nature of metal salts, solvents, pH of the reaction medium and mole ratio of reactants also contribute to the overall nature of the complexes. The metal complexes of dihydrazones are well known to have significant pharmacological applications such as antimicrobial, anti-inflammatory and antitumor activities rendering their tremendous potential in drug design and so have attracted many researchers in their study [1,6]. Moreover, they also serve as catalysts, electrocatalysts, analytical and industrial chemistry with applications in diverse fields [7].

In this study, ligand *bis*(2-hydroxy-1-naphthaldehyde)-glutaryldihydrazone ($naghH_4$) was derived from the condensation of *o*-hydroxy aromatic aldehyde and acyldihydrazine by a simple synthetic procedure. This bulky multidentate ligand $naghH_4$ possesses two hydrazone arms joined through three intervening methyl groups that offer the flexibility of free rotation about the C-C single bond with the possibility of preferential stereochemical disposition depending on the metal valences and the nature of bonds. It has been found that the presence of N-C=O moiety improves the biological efficacy of the hydrazone based metal complexes [3]. Many studies have also attributed their chemical and biological properties to the significant role of the trigonally hybridized nitrogen

atoms of the azomethine groups (-CH=N) with lone pair of electrons [7]. The literature survey revealed that a series of transition metal complexes of dihydrazones have been studied however complexes of *bis*(2-hydroxy-1-naphthaldehyde)glutaryldihydrazone ($naghH_4$) have not yet been much explored . To the best of our knowledge, less studies of metal complexes of disalicylaldehyde glutaryldihydrazone [8] are known.

Manganese(IV) complexes with Schiff bases are of significant interest as they are potential candidates for models of enzymes as biomimics [9]. Many studies have proposed that a mononuclear manganese(IV) center present at the active site of some enzymes assist superoxide dismutase activity [10]. In addition, studies have identified the fundamental role of Mn in higher oxidation states like Mn(III) and Mn(IV) in biological redox processes as an oxygen-evolving center of photosystem II (PSII OEC) in green plants when water is oxidized to oxygen molecule [5,11], wherein the embedded tetramanganese complexes (the oxygen-evolving complex, OEC) perform as electron donors [2,11]. Besides its implication in a number of biological processes, it is also known to be involved as single molecular magnets [12], oxidizing agents, catalysts, electrocatalysts, aliphatic and aromatic C-H activation and oxygen insertion reactions [13]. Thus, the higher oxidation state of manganese has attracted tremendous attention with potential applications in several fields [13]. Moreover, the manganese complexes are generally known to have a less toxic effect on the environment [9]. It is worth mentioning that the literature survey has revealed that not many dihydrazone complexes of Mn(IV) have been documented to date. Notably, the manganese coordination chemistry is majorly dominated by the more stable form of manganese in +2 and +3 oxidation states [4].

In the present work, pyridine and its derivatives have preferentially been incorporated as auxiliary ligands. They also bear immense biological interest as many of these are known to be part of several biological molecules such as enzymes, alkaloids, *etc*. and have wide applications in the pharmaceutical industry [14]. We herein report, the synthesis, physico-chemical studies, spectroscopic characterization, electrochemical behaviour and antimicrobial activity of *bis*(2-hydroxy-1-naphthaldehyde)-glutaryldihydrazone and its manganese(IV) complexes.

EXPERIMENTAL

The chemicals used in this study *viz*. $Mn(OAc)_2{\cdot}4H_2O$, diethyl glutarate, hydrazine hydrate and 2-hydroxy-1-naphthaldehyde were of E-Merck or equivalent grade. Analysis of manganese was performed by following the standard procedure [15]. Microanalysis C, H, N of few complexes were determined with EuroEA elemental analyzer. Systronics Direct Reading Conductivitymeter-303 with dip-type conductivity cell was used to measure molar conductances of the metal complexes for 4×10^{-3} M concentration in DMSO at room temperature. Sherwood Scientific Magnetic Susceptibility Balance was used to measure magnetic susceptibility using $Hg[Co(SCN)_4]$ as calibrant at room temperature. ESI-MS spectrum was recorded using Agilent 6520 Quadrupole-TOF mass spectrometer. The melting point and decomposition temperatures were measured using Analab Scientific instruments. EPR spectral data were recorded in X-band frequency at liquid nitrogen temperature (LNT) and room temperature (RT) in DMSO solvent using JES-FA200 ESR spectrometer. IR spectral data were obtained from Spectrum 2 Perkin-Elmer FTIR spectrometer with KBr disks. The electronic spectra were recorded on Perkin-Elmer Lambda 35 UV-Vis spectrophotometer from 250 to 800 nm in DMSO solvent. Thermal stability and decomposition of the analytical complexes were determined by means of Mettler-Toledo thermal analyzer system recording TGA and DTG curves in the temperature range 25-700 ºC under N_2 atmosphere with a heating rate of 20 ºC min^{-1}. The electrochemical studies were carried out on CHI660D CH instrument electrochemical workstation. The electrolytic cell consisted of three electrodes: reference electrode as Ag/AgCl, working electrode as Pt disk and Pt wire as auxiliary electrode.

Synthesis of ligand: A mixture of diethyl glutarate (4.08 g, 21.67 mmol) in methanol (10 mL) was reacted with hydrazine hydrate (2.12 g, 42.35 mmol) in methanol (10 ml) at 1:2 molar ratio to synthesize glutarohydrazide. This was followed by condensation of glutarohydrazide (0.7 g, 4.37 mmol) with 2-hydroxy-1-naphthaldehyde (1.5 g, 8.71 mmol) in methanol medium (10 mL) at a molar ratio of 1:2 by stirring for 1 h at room temperature and refluxing for another 1 h. *bis*-(2-hydroxy-1-naphthaldehyde)glutaryldihydrazone ($naghH_4$) was obtained as an off-white precipitate. It was washed thoroughly with methanol, then filtered and finally dried over anhydrous $CaCl_2$ (D.P. >250 ºC).

Synthesis of complex (1): For the synthesis of complex $[Mn^{IV}(nagh)(H_2O)_2)]{\cdot}2H_2O$ (**1**), $naghH_4$ (0.466 g, 1 mmol) was dissolved in methanol (25 mL) followed by dropwise addition of methanolic solution of $Mn(OAc)_2{\cdot}4H_2O$ (0.245 g, 1 mmol) at a molar ratio of 1:1. The mixture was stirred for 30 min at room temperature and then gently refluxed for 2 h. The reaction was allowed to cool, filtered and then a pale olive green coloured product that was obtained was washed several times with hot methanol and water, and finally dried over anhydrous $CaCl_2$ (yield = 81.2%) (**Scheme-I**).

Synthesis of complexes (2-7) : To the above reaction mixture of $Mn(OAc)_2{\cdot}4H_2O$ and $naghH_4$, pyridine or a pyridine base (2-picoline, 3-picoline, 4-picoline, 2,2′-bipyridine or 1,10-phenanthroline) was added maintaining a molar ratio at 1:1:10 of $Mn(OAc)_2{\cdot}4H_2O$:$naghH_4$:pyridine/pyridine base or at molar ratio of 1:1:2 for 2,2′-bipyridine or 1,10-phenanthroline and refluxed for an hour, cooled, filtered and washed thoroughly with hot methanol and water, then dried over anhydrous $CaCl_2$. The following products were isolated: $[Mn^{IV}(nagh)(A)_2)]{\cdot}2H_2O$ [A= (py, **2**); (2-pic, **3**); (3-pic, **4**) and (4-pic, **5**)] and $[Mn^{IV}(nagh)(NN)]$ (NN = (bpy, **6**) and (phen, **7**)] (yield: 71% (**2**); 78% (**3**); 63% (**4**,**5**); 67% (**6**) and 74% (**7**) (**Scheme-I**).

Antibacterial activity: The antibacterial studies were conducted using pour plate method. In brief, sterile Mueller Hinton agar media was transferred into the petri dishes and instantly enclosed by a lid. The plates were cooled and left inverted and then incubated. A loop with bacterial culture was added to the nutrient broth and incubated at 37 ºC for 24 h. The 24 h culture of tested bacteria was aseptically transferred to sterile agar petri plates and then the inoculums were spread

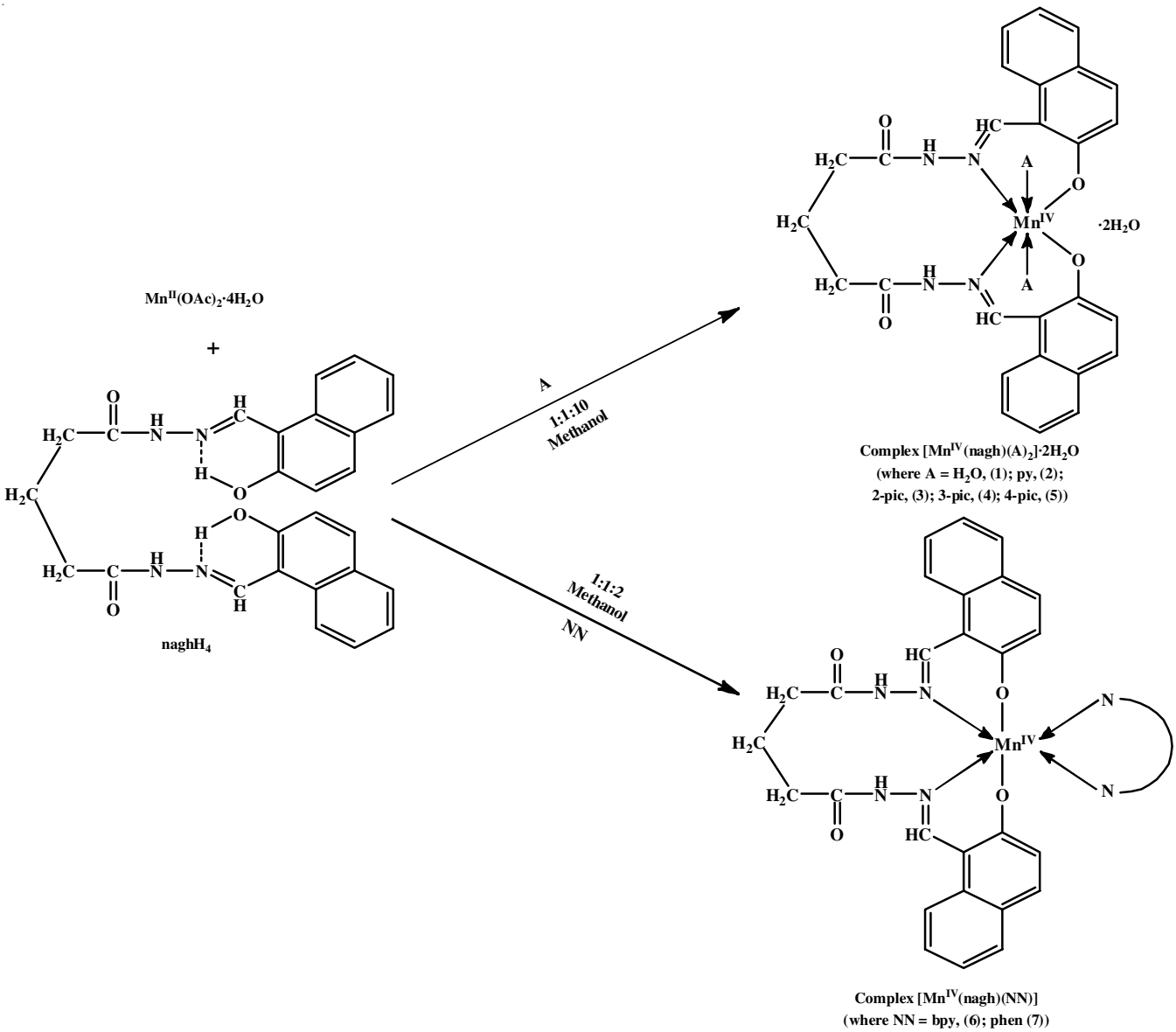

Scheme-I: Synthetic route of the manganese(IV) complexes

over agar plates using a sterile spreader. Four bores were prepared on the agar plates using 6 mm sterile borer. Then, 0.1 mL of each ligand and manganese(IV) complexes dissolved in 5% DMSO were distributed into the labeled bores that were marked at the back of plates. Each plate consisted of a bore for 5% DMSO as control was then incubated at 37 ºC for 48 h. The plates were then observed after 24 h for the development of inhibition zone and then the diameter of inhibition zones were measured.

RESULTS AND DISCUSSION

The analytical data and physical properties of the synthesized manganese complexes are summarized in Table-1. These complexes are not hygroscopic and do not dissolve in water as well as in organic solvents like methanol, ethanol, acetone, *etc*. but are soluble in DMSO and DMF. The synthesized manganese(IV) complexes do not decompose up to 250 ºC indicating the strong bonding and higher ionic character. Their insolubility in many solvents have made crystallization of these complexes difficult. Nevertheless, several attempts were made but failed preventing us from analyzing their molecularity and structure using X-ray crystallography.

Molar conductance : The molar conductance values in the range of 1.8-4.9 $ohm^{-1}\,cm^2\,mol^{-1}$ in DMSO at 10^{-3} mol L^{-1} dilution for these complexes correspond to their non-electrolytic nature (Table-1) [4,13,16].

Magnetic moment : The μ_{eff} values for these complexes are listed in Table-1, which fall in the range 3.49-4.34 B.M. and are consistent with octahedral mononuclear Mn(IV) complexes having d^3 electronic configuration [2,4,13].

IR spectra : The key IR bands of free ligand and its Mn(IV) complexes are tabulated in Table-2. The IR spectra of the free ligand and its manganese complexes (**1** and **2**) are displayed as representatives in Fig. 1. The ν(C=O) band of dihydrazone was observed as two strong peaks at 1669 and 1644 cm^{-1} [13]. The disappearance of these stretching frequencies of carbonyl

TABLE-1
COLOUR, DECOMPOSITION POINT, ANALYTICAL, MAGNETIC MOMENT AND MOLAR CONDUCTANCE (Λ_m) DATA OF Mn(IV) COMPLEXES OF $naghH_4$

Complex	Colour	D.P. (°C)	Elemental analysis (%): Found (calcd.)				μ_{eff} (B.M.)	Λ_m (ohm^{-1} m^2 mol^{-1})
			Mn	C	H	N		
$[Mn^{IV}(nagh)(H_2O)_2]\cdot 2H_2O$	Pale olive green	> 250	9.19 (9.29)	50.11 (54.83)	4.40 (4.77)	12.31 (9.47)	3.49	1.8
$[Mn^{IV}(nagh)(py)_2]\cdot 2H_2O$	Pale olive green	> 250	7.41 (7.33)	60.31 (59.28)	4.51 (5.10)	14.61 (11.21)	4.13	2.5
$[Mn^{IV}(nagh)(2\text{-}pic)_2]\cdot 2H_2O$	Pale olive green	> 250	7.29 (7.05)	61.49 (60.07)	4.96 (5.69)	13.88 (10.78)	4.34	3.1
$[Mn^{IV}(nagh)(3\text{-}pic)_2]\cdot 2H_2O$	Pale olive green	> 250	7.41 (7.05)	– (60.07)	– (5.69)	– (10.78)	3.70	2.8
$[Mn^{IV}(nagh)(4\text{-}pic)_2]\cdot 2H_2O$	Pale olive green	> 250	7.33 (7.05)	– (60.07)	– (5.69)	– (10.78)	3.90	2.3
$[Mn^{IV}(nagh)(bpy)]$	Yellowish brown	> 250	6.46 (8.14)	– (65.78)	– (4.18)	– (12.44)	4.21	4.1
$[Mn^{IV}(nagh)(phen)]$	Light brown	> 250	5.89 (7.85)	– (66.95)	– (4.03)	– (12.01)	3.85	4.9

TABLE-2
KEY INFRARED STRUCTURAL BANDS (cm^{-1}) OF $naghH_4$ AND ITS MONOMETALLIC MANGANESE(IV) COMPLEXES

Ligand/ complex	ν(OH) + ν(NH)	ν(C=O)	ν(C=N)	Amide(II) + ν(C–O) naphtholic	β(C–O) naphtholic	ν(N–N)	ν(M–O) naphtholic	ν(M–N) azomethine	ν(M–N) in-plane ring deformation	ν(M–N) py
$naghH_4$	3000-3685(mbr) 3436(mbr) 3187(m) 3048(m)	1669(s) 1644(s)	1627(s) 1602(s)	1579(s)	1282(m)	1032(w)	–		–	
1	3000-3600(sbr) 3413(sbr) 3188(s) 3048(s)	–	1617(s) 1601(s)	1582(s) 1540(s)	1250(m)	1039(w)	561(w) 543(w)		–	
2	3000-3600(sbr) 3420(sbr) 3188(sbr) 3044(sh)	–	1616(s) 1602(s)	1583(s) 1537(s)	1250(m)	1039(w)	561(w) 543(w)	362(s)	650(w)	295(s)
3	3000-3600(sbr) 3420(sbr) 3188(sbr) 3048(s)	–	1616(s) 1602(s)	1583(s) 1537(s)	1249(m)	1038(w)	560(w) 543(w)		640(w)	
4	3000-3600(sbr) 3486(wbr) 3155(mbr) 3037(msh)	–	1616(s) 1602(s)	1583(s) 1537(s)	1250(m)	1030(w)	560(w) 543(w)		650(w)	
5	3000-3650(sbr) 3481(sbr) 3165(sbr) 3034(msh)	–	1616(s) 1601(s)	1585(s) 1537(s)	1249(m)	1030(w)	560(w) 543(w)		650(w)	
6	3000-3650(sbr) 3441(sbr) 3188(sbr) 3038(msh)	–	1616(s) 1602(s)	1583(s) 1537(s)	1249(m)	1037(w)	560(w) 543(w)		649(w)	
7	3000-3650(sbr) 3438(sbr) 3188(mbr) 3044(mbr)	–	1616(s) 1601(s)	1583(s) 1537(s)	1249(m)	1036(w)	560(w) 544(w)		651(w)	

bands in the complexes indicated destruction of amide groups and chelation of dihydrazone to the manganese center in the *enolic* form [4,5,13]. The peaks at 1627 and 1602 cm^{-1} are characterized by ν(C=N) bands [9,17,18]. These stretching vibrational bands remain almost unshifted in position or show a small shift to a lower frequency by an average of 5 cm^{-1} in the complexes. This feature of ν(C=N) band endorses the difference of bonded species (H^+ or M^{4+}) to the C=N groups and is correlated to bonding through imine nitrogen to the manganese center [17].

A strong band at 1579 cm^{-1} in dihydrazone is associated with its composite character from mixed contribution of amide II and ν(C–O)(naphtholic) bands. This band splits into two stronger bands between the ranges of 1585-1537 cm^{-1} which suggest contribution from the newly created NCO^- group due to deprotonation of enolized carbonyl group [4,13]. A negative shift of the band to lower frequency by 17 to 18 cm^{-1} in these complexes also indicate chelation of naphtholate oxygen atoms to the metal center. A medium intensity peak at 1282 cm^{-1} is related to phenol/naphthol group in several dihydrazones and hence assigned here to β(C-O) naphtholic group [5,18]. This peak shifts to lower frequency by 32-33 cm^{-1} indicating a bonding of naphtholate oxygen to the metal center [18]. The shift of β(C-O)(naphtholic) band to lower frequency in the complexes is associated with flow of π-electron density of aromatic ring to metal center through the azomethine group [5].

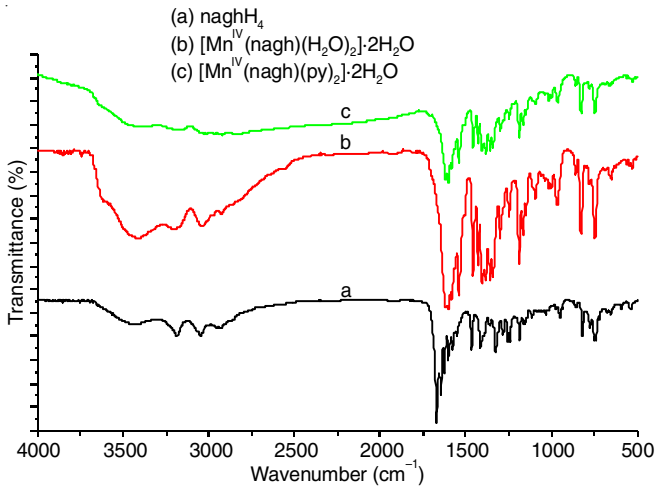

Fig. 1. Infrared spectra of ligand (a) naghH$_4$ and complexes (b) [Mn^{IV}(nagh)(H$_2$O)$_2$]·2H$_2$O (**1**) (c) [Mn^{IV}(nagh)(py)$_2$]·2H$_2$O (**2**)

A characteristic ν(N–N) band observed at 1032 cm^{-1} as weak intensity band in free dihydrazone remain as weak bands in complexes between 1039-1030 cm^{-1} with almost unshifted or small shift to higher frequency that provides an evidence for chelation of only one hydrazine nitrogen atom to the metal ion [2]. The medium intensity band in the region 3187-3048 cm^{-1} in dihydrazone is attributed to ν(N-H) stretching vibrations, which remain unchanged or is shifted to lower wavenumber side falling in the region 3188-3034 cm^{-1} in the complexes, which corresponds to non-involvement of the nitrogen atom of –NH group.

An existence of non-ligand peaks at 561-543 cm^{-1} and 362 cm^{-1} in the complex **2** (representative complex) may be attributed to ν(M-O)$_{naphtholate}$ and ν(M-N)$_{azomethine}$ bands, respectively [12,13,19,20], which suggest bonding of ligand to the metal *via* naphtholate oxygen and azomethine nitrogen atoms in these complexes [6]. A presence of peak at 604 cm^{-1} corresponds to in-plane ring deformation mode of pyridine [13]. Hence, the new weak intensity bands observed in the region 651-640 cm^{-1} in the complexes **2-7** were assigned to in-plane ring deformation mode of pyridine or pyridine bases on coordination to the metal center [19]. Also, a new strong band at 295 cm^{-1} in complex **2** is assigned to ν(Mn-N) due to coordinated pyridines [21].

A broad medium intensity band in the region 3307-3681 cm^{-1} and centered at 3436 cm^{-1} in free dihydrazone is assignable to the stretching vibration of naphtholic –OH with intramolecular bonding (O-H…N) [6,18]. Replacement of this band by a much broader absorption band centered in the region 3486-3413 cm^{-1} in complexes **2-5** is proposed due to antisymmetric and symmetric stretching –OH vibrations of lattice water molecule while this broad band in the above region in complex **1** is suggested to also have contribution from the coordinated water molecules as is also corroborated from the TGA data. A new weak intensity peak observed at 659 cm^{-1} in complex **1** is attributed to the rocking mode of the water molecules coordinated to the metal center [22]. The spectra of these complexes exhibited a new hump or shoulder of weak to medium intensity in the region 3684-3613 cm^{-1}, which may also be related to strong H-bonding by the enolate C-O group with the associated water molecule in lattice or coordinated form and/or the secondary –NH group. The weak bands between 3038-2800 cm^{-1}, region are identified as symmetric and asymmetric modes of the –CH and –CH$_2$ groups [19].

Evidently, the appearance of ν(C=N) [9], amide(II) + νCO$_{(naphtholic)}$ and ν(Mn-O)$_{naphtholic}$ stretching vibrations in the form of couple of bands in the IR spectra of these complexes indicate inequivalent hydrazone arms of the dihydrazone with unequal lengths of bonds that correspond to chelation of dihydrazone to the same metal center in *anti-cis* configuration [4,13]. In such configuration, one hydrazone arm attains axial position while the other hydrazone arm remains in the equatorial position [4,13].

Thermal studies: The IR spectral data of complexes (**1-5**) indicated the presence of water molecules, following which, the thermal analyses (TGA) was carried out to determine their nature. The complexes (**6** and **7**) have not indicated any presence of water molecules in the lattice or in coordinated structure. The thermogravimetric analysis of complexes **1**, **2** and **3** were studied as representative samples at room temperature of up to 700 ºC at a heating rate of 20 ºC/min. The temperature intervals and percentage loss of masses of complexes **1-3** are summarized in Table-3. The TG/DTG curve of complex **1** is depicted in Fig. 2, where thermal decomposition in four stages is observed. In the first degradation stage, weight loss of 13.42% (calcd. 13.77%) occurred between 34-200 ºC. This weight loss corresponds to the liberation of two lattice and two coordinated water molecules. The associated DTG peak is observed at 71 ºC. The second stage of degradation occurred between 200-386 ºC with a weight loss of 29.41% (calcd. 29.07%). The related DTG peak is observed at 367 ºC due to loss of $C_5H_8N_4O_2$ moiety. The third stage show one degradation between 386-420 ºC with a weight loss of 8.49% (calcd. 9%) that correspond to the loss of four –CH fragment with DTG peak at 414 ºC. The fourth degradation step exhibits weight loss at 420-580 ºC. The DTG curve is centered at 502 ºC indicating the maximum weight loss. The total weight loss was found to be 63.84% as against the calculated value of 64.84%. Subsequent mass loss of 3.51% continues with TGA curve proceeding down up to the recorded temperature of 700 ºC when a residue of mass 33.08% is finally left which could be a metallic oxide residue.

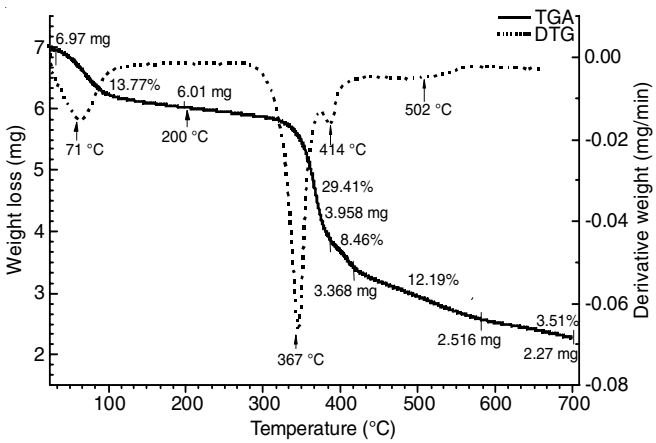

Fig. 2. TGA and DTG curves of [Mn^{IV}(nagh)(H$_2$O)$_2$]·2H$_2$O (**1**)

TABLE-3
THERMOANALYTICAL RESULTS (TG AND DTG) OF MANGANESE(IV) COMPLEXES OF naghH$_4$

Complexes	TG range (°C)	DTG (°C)	Found (calcd.) (%)		Assignment
			Mass loss	Total mass loss	
$[Mn^{IV}(nagh)(H_2O)_2]\cdot 2H_2O$ (**1**)	34-200	71	13.42 (13.77)	63.84 (64.84)	Loss of two lattice & two coordinated H_2O molecules
	200-386	367	29.41 (29.07)		Loss of organic moiety ($C_5H_8O_2N_4$)
	386-420	414	8.49 (9.00)		Loss of organic moiety 4(-CH)
	420-580	502	12.19 (13.00)		Loss of organic moiety (-C_6H_3)
$[Mn^{IV}(nagh)(py)_2]\cdot 2H_2O$ (**2**)	32-192	56	6 (5.46)	60.85 (59.38)	Loss of two lattice H_2O molecule
	192-303	246	2		
	303-400	388	33.35 (34.34)		Loss of two pyridine molecule & C_4H_6O
	400-428	422	9.53 (8.80)		Loss of CON_2H_2
	428-544	497	7.48 (8.2)		Loss of $C_2H_2N_2$
	544-614	570	2.49 (2.58)		Loss of OH
$[Mn^{IV}(nagh)(2\text{-pic})_2]\cdot 2H_2O$ (**3**)	39-136	85	8.78 (7.45)	54.29 (54.25)	Loss of two lattice H_2O molecule & CH_3
	136-398	373	23.97 (23.97)		Loss of two pyridine base molecules
	398-423	414	7.86 (8.20)		Loss of $C_2H_2N_2$
	423-447	430	1.69 (2.58)		Loss of OH
	447-648	520	11.96 (13.00)		Loss of C_6H_3

The TGA curve of complex **2** showed rapid first step decomposition in the temperature range 32-192 ºC with a 6% mass loss (calcd. 5.46%) indicating the loss of two lattice water molecules with a DTG peak at 56 ºC. The second stage with two degradation steps occurred at the temperature range 192-400 ºC accompanied by two DTG peaks, one a very weak peak at 246 ºC and another a very strong peak at 388 ºC. The combined weight loss of 35.353% (calcd. 34.34%) corresponds to the simultaneous losses of two pyridine moieties and another C_4H_6O moiety. This was followed by decomposition steps at the temperature ranges of 400-428, 428-544 and 544-614 ºC with DTG peaks at 422, 497 and 570 ºC, respectively. The corresponding weight losses of 9.53% (calcd. 8.80), 7.48 % (calcd. 8.2%) and 2.49% (calcd. 2.58 %) in these temperature ranges are due to losses of CON_2H_2, $C_2H_2N_2$ and OH. Thus, within the temperature range of 32-614 ºC, an overall weight loss of 60.85% (calcd. 59.38%) was found. The TGA curve extends downward up to 700 ºC with an estimated 34.42% residue remaining after this temperature.

In complex **3**, the first stage of degradation occurred between 39-136 ºC with a weight loss of 8.78% (calcd. 7.45%). This weight loss corresponds to the simultaneous loss of two lattice water and CH_3 with associated DTG peak at 85 ºC. The second stage degradation occurred at 136-398 ºC with a weight loss of 23.97 (calcd. 23.97%). This weight loss corresponds to the loss of two C_5H_5N moieties with the DTG peak at 373 ºC. The third stage proceeded within the temperature range 398-423 ºC with a weight loss of 7.86% (calcd. 8.2%) that corresponds to the loss of $C_2H_2N_2$ fragment with DTG peak at 414 ºC. The fourth and fifth degradation steps occurred within the temperature ranges of 423-447 and 447-648 ºC, respectively. The weight losses of 1.69% (calcd. 2.58%) and 11.96% (calcd. 13%) within these temperature ranges corresponds to the losses of OH and C_6H_3 with DTG peaks at 430 and 520 ºC, respectively. The overall weight loss of 54.29% (calcd. 54.25%) was estimated between the temperature range of 39-520 ºC. The TGA curve proceeded downward up to 700 ºC and the remaining residue at this temperature is estimated to amount to 44.12%.

In brief, complexes **1**-**3** displayed a TGA peak in the range 32-200 ºC temperature range that were correlated with the weight loss of two lattice water molecules. In complex **1**, the weight loss from 34 ºC to 200 ºC was assigned to two lattice and two coordinated water molecules [23]. The complexes **2** and **3** showed a weight loss in the temperature range of 136-400 ºC corresponding to two pyridine and 2-picoline molecules, respectively [14].

Mass spectrum: The ESI-MS spectrum of complex **2** was studied as a representative sample. It showed a molecular ion peak, *m/z* at 556.4011, which may be due to the formation of $[Mn(nagh\text{-}C_3H_3)]^+$ species. The fragmentation peaks at *m/z* 570.4173, 578.3832 and 592.3991 may be attributed to cleavage of the complex and formation of $[Mn(nagh\text{-}C_4H_5)]^+$, $[Mn(nagh\text{-}C_3H_{11}N)]^+$ and $[Mn(nagh\text{-}C_4H_{13}N)]^+$ species, respectively, are well observed in its mass spectrum. These signals that are attributed to different chemical species are indicative of the composition of this complex and it's monomeric nature [24].

Electronic spectra: The electronic spectral values of dihydrazone and its manganese complexes in DMSO solutions are given in Table-4 along with their molar extinction coefficients and the spectra of ligand and its complexes **1**, **3** and **7** are displayed as representative complexes in Fig. 3. The ligand bands in the range of 282-328 nm may be attributed to π-π* transition while the bands in the range of 357-410 nm may be attributed to n-π* transitions. The bands above ~340 nm are a distinguished feature of naphthyl rings as has been reported in several monoacyl/arylhydrazones [25].

The ligand bands at 282 and 288 nm in the complexes undergo no shift or a slight red-shift by 1-4 nm with increase in intensity and formation of another band at 291 nm is observed in the complexes **6** and **7**. The ligand band at 310 nm dissappeared in the complexes. A weak shoulder at 310 nm is however detectable in the complexes **2** and **3** but is absent in the other complexes. The ligand band at 322 nm is broadened and red-shifted by 1-6 nm in these complexes. The strong ligand bands at 357 nm and 369 nm also disappeared in complexes **4** to **7** but is observable as a weak shoulder in the complexes **1**-**3** at 377 nm. The weak ligand band at 410 nm (ε = 350 M^{-1} cm^{-1})

TABLE-4
ELECTRONIC SPECTRAL BANDS AND EPR DATA FOR MANGANESE(IV) COMPLEXES OF $naghH_4$

Ligand/ Complex	λ_{max} (nm) (ε_{max}) ($dm^3\ mol^{-1}\ cm^{-1}$)	Temp.	Solid/ solution	g-value	A_{Mn} value (G)
$naghH_4$	282 (3624), 288 (2583), 310 (7307), 322 (9476), 357 (8687), 369 (8641), 410 (350)				
1	282 (3689), 288 (3485), 324 (4468), 377sh (249), 410 (4974), 430 (5532)	LNT	DMSO	2.0029	90
		RT	DMSO	2.0157	–
2	282 (3880), 288 (3614), 310sh (3814), 324 (4711), 377sh (2851), 411 (4441), 430 (4750)				
3	282 (4216), 288 (3814), 310sh (4030), 323 (4849), 377sh (2864), 411 (4669), 430 (5072)	LNT	DMSO	1.9747	83.332
		RT	DMSO	2.001	–
4	282 (4401), 288 (4216), 328 (5963), 410 (6986), 429 (7654)				
5	284 (3827), 292 (5490), 328 (8074), 411 (9342), 430 (10000)				
6	281 (3819), 287 (3670), 291 (3972), 325 (5855), 410 (6352), 430 (6855)				
7	282 (3598), 287 (3627), 291 (3224), 326 (4476), 411 (4823), 431 (5154)	LNT	DMSO	1.9949	94.0303
		RT	DMSO	2.0433	–

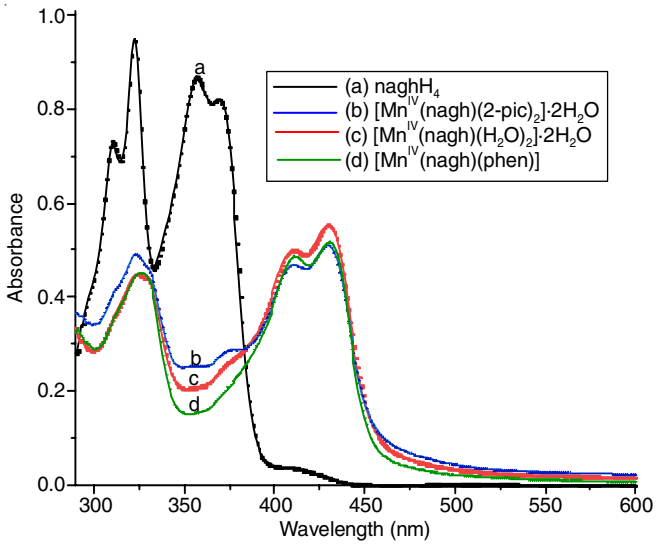

Fig. 3. Electronic spectra of ligand (a) $naghH_4$ and complexes (b) $[Mn^{IV}(nagh)(2\text{-pic})_2]\cdot 2H_2O$ (**3**) (c) $[Mn^{IV}(nagh)(H_2O)_2]\cdot 2H_2O$ (**1**) (d) $[Mn^{IV}(nagh)(phen)]$ (**7**)

remained almost unshifted in these complexes falling in the range 410 or 411 nm but exhibited a very large increase in intensity with ε value in the range of 4441-9342 $M^{-1}\ cm^{-1}$. In addition to these intra-ligand bands, a new band of high intensity at 429-431 nm with ε value in the range of 4750-10,000 $M^{-1}\ cm^{-1}$ are observed in these complexes.

Manganese(IV) complexes in an octahedral environment exhibit three possible spin-allowed *d–d* transitions: $^4A_{2g}\rightarrow{}^4T_{2g}$, $^4A_{2g}\rightarrow{}^4T_{1g}(F)$ and $^4A_{2g}\rightarrow{}^4T_{1g}(P)$ [13,17,26]. The additional band observed in the region 429-431 nm cannot be assigned to *d–d* transition because it has a high value of molar extinction coefficient than those expected for *d–d* bands that lie almost in the same range of ε_{max} values which have been reported by Cooper *et al.* [27] and Okawa *et al.* [28] for Mn(IV) complexes, which they had attributed to LMCT transitions. Hence, it may be assigned to charge transfer band [28]. Also, the band at 410-411 nm with high molar extinction coefficients may be dominated by the charge transfer band since it has a very large molar extinction coefficient value that may be due to contribution of charge-transfer from ligand-to-metal probably from naphtholic oxygens to *d*-orbital of Mn(IV) ions [13,28,29].

EPR spectra: The EPR magnetic parameters for complexes **1**, **3** and **7** at liquid nitrogen temperature (LNT) and room temperature (RT) in DMSO are shown in Table-4. The EPR spectra of these complexes show an isotropic signal with g values in the range of 1.9747-2.0433. Complexes **1** and **3** exhibited similar spectral features both at LNT and RT in DMSO. At LNT in DMSO, they showed spectral features with detectable hyperfine structures, which are not very well-defined and the Mn hyperfine splitting constants are 90 and 83.332 G for the complexes **1** and **3**, respectively. The shape of EPR signal for complex **7** is different from that of the complexes **1** and **3**. The intensity of the signal at g = 1.9949 for this complex is weak with hyperfine structure (A = 94.0303 G). The Mn hyperfine splitting constants authenticated the presence of Mn(IV) complexes for a d^3 ion that has $^4A_{2g}$ ground states with S = 3/2 in an octahedral geometry [4,13]. In all these three cases, there are weak forbidden transitions that are observable between the hyperfine sextets at LNT. At RT in DMSO, these three complexes exhibit a broad component in the range between ~2500-3500 G. The zero-field splitting parameters are indicative of the structural properties for S > ½ systems. With $^4A_{2g}$ ground term, a Mn(IV) compound display isotropic metallic center with a strong signal at ~g = 2 which is a characteristic of an octahedral symmetric mononuclear Mn(IV) species with D = 0 [12,17,29].

Cyclic voltammetry: The electron transfer processes of the dihydrazone and its Mn(IV) complexes **1** and **3** in DMSO (2 mmol) using TBAP as a supporting electrolyte under nitrogen atmosphere at room temperature were investigated by cyclic voltammetry (CV). The CVs of Mn(IV) complexes were studied over the potential window of +1.5 to -1.5 V at 100 mV/s scan rate (Table-5). The uncoordinated dihydrazone displayed two redox couples at -0.35 V ($E_{1/2}$) (ΔE = 240 mV) and +0.24 V ($E_{1/2}$) (ΔE = 130 mV), which apparently are quasireversible and an irreversible anodic peak potential at +0.841 V was observed. The free ligand is electroactive [30] while the complexes **1** and **3** do not show any metal-centered redox peaks. The features of cathodic and anodic peaks in complexes (**1**) and (**3**) suggest that these are ligand-based redox processes having slight negative shifts in peak positions and exhibiting similar peak intensity [31]. The CV of complex **1** is shown in Fig. 4. The

TABLE-5
ELECTROCHEMICAL DATA FOR THE LIGAND AND ITS MANGANESE(IV) COMPLEXES (Pot. *vs.* Ag/AgCl) AT SCAN RATE OF 100 mV/s

Ligand/Complex	Anodic peak potential E_{pa} (V)	Cathodic peak potential E_{pc} (V)
$naghH_4$	–0.232	–0.473
	+0.312	+0.175
	+0.841	–
$[Mn^{IV}(nagh)(H_2O)_2]\cdot 2H_2O$ (**1**)	–0.181	–0.472
	+0.291	+0.171
	+0.828	–
$[Mn^{IV}(nagh)(2\text{-pic})_2]\cdot 2H_2O$ (**3**)	–0.180	–0.443
	+0.147	+0.129
	+0.820	–

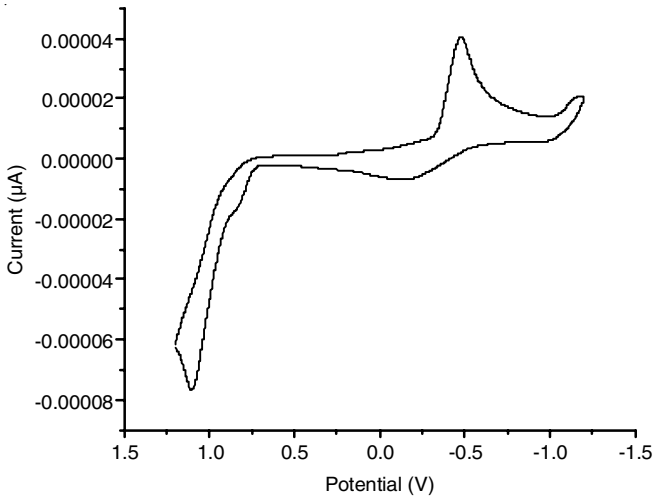

Fig. 4. Cyclic voltammogram of complex $[Mn^{IV}(nagh)(H_2O)_2]\cdot 2H_2O$ (**1**)

shifts in peak potential show a decrease in going from complex **1** to complex **3** indicating the donor influence of water and the pyridine based molecule.

Antibacterial susceptibility test: The *in vitro* antibacterial properties of the dihydrazone and its manganese(IV) complexes were evaluated against *Staphylococcus epidermis* (MTCC 435), *Bacillus cereus* (MTCC 1305), *Klebsiella pneumonia* (MTCC 10309), *Escherichia coli* (MTCC 1669), *Enterobacter aerogenes* (MTCC 8559) and *Proteus vulgaris* (MTCC 426) bacteria by standard Agar well diffusion method [32]. The complexes **1**, **2**, **6** and **7** were allowed to diffuse through the agar gel previously inoculated with a test bacterial pathogen. After incubation of the plates for 24-48 h, the bacterial colonies showed a growth wherever possible and produced a haze in the agar. The microorganism served as indicator, for visibility and activity of the complexes. Clear inhibition zone observed near the agar well in the plates indicated limited growth of the microorganisms [32]. The 5% DMSO solvent used was also tested as negative control in order to ascertain that the antimicrobial activity was not due to the solvent.

The observed zone of inhibition against different bacteria were measured and tabulated as shown in Table-6. The results of this study showed that the ligand has slight antibacterial activity against Gram-negative bacteria, *Enterobacter aerogenes* (MTCC 8559) and *Proteus vulgaris* (MTCC 426). The metal complexes **6** and **7** showed moderate antibacterial activity against the Gram-negative bacteria *Enterobacter aerogenes* (MTCC 8559) and high activity against *Proteus vulgaris* (MTCC 426) with an inhibition zone of more than 8 mm.

Bakare [33] had earlier reported that the presence of azomethine group is important for antibacterial activity of Schiff bases and the chelation effect in metal chelates enhances their activity as can be explained based on chelation theory [25]. Besides, the incorporation of pyridine moieties in the structural unit of the complexes is also known to induce potency against pathogenicity [14]. Based on the data shown in Table-6, it may be proposed that complexes **1** and **2** with monodentate auxiliary ligand are not effective as antibacterial while the complexes **6** and **7** with bidentate auxiliary ligand are active and more effective than the free ligand on the two Gram-negative bacteria, *E. aerogenes* and *P. vulgaris*. However, the free ligand and its manganese(IV) complexes do not show any activity against the Gram-positive bacteria (*S. epidermis* and *B. cereus*) and the other two tested gram-negative bacteria *K. pneumonia* and *E. coli*.

It is worth to mention that Gram-negative bacteria are mostly very difficult to treat which is ascribed to their restrictive membrane [34]. Moreover, it is reported that antimicrobials with efficacy towards the Gram-negative bacteria are in general found to be also effective for antitumour activity [34]. Hence, the complexes **6** and **7** seems to be a good candidate for further investigations on its biological activities.

Conclusion

In this study, the structural investigation, redox behaviour and antimicrobial potentials of *bis*(2-hydroxy-1-naphthalde-

TABLE-6
ANTIMICROBIAL STUDIES OF THE LIGAND $naghH_4$ AND ITS MANGANESE(IV) COMPLEXES

Schiff base/ Complexes	Zone of inhibition (mm)					
	Gram-positive bacteria		Gram-negative bacteria			
	Staphylococcus epidermis MTCC-435	*Bacillus cereus* MTCC-1305	*Klebsiella neumonia* MTCC-10309	*Escherichia coli* MTCC-1669	*Enterobacter aerogenes* MTCC-8559	*Proteus vulgaris* MTCC-426
Ligand	–	–	–	–	03^{+}	04^{+}
1	–	–	–	–	–	–
2	–	–	–	–	–	–
6	–	–	–	–	06^{++}	12^{+++}
7	–	–	–	–	08^{++}	10^{+++}

Highly active = +++ (inhibition zone > 8.2 mm); Moderately active = ++ (inhibition zone > 5.0-8.2 mm); Slightly active = + (inhibition zone > 2.5-5.0 mm); Inactive = – (inhibition zone < 2.5 mm)

hyde)glutaryldihydrazone ($naghH_4$) and seven new mononuclear manganese(IV) complexes derived from $naghH_4$ are reported. The reactions performed under open atmosphere have probably facilitated this electron-rich deprotonated ligand to stabilize the high oxidation state of manganese in these complexes using aerial oxygen as the oxidizing agent. The free dihydrazone coordinated to Mn(IV) ion with its tetradentate NNOO donors. The dihydrazone exist in enolic form in all these complexes and is proposed to be arranged such that the donors from the ligand are present around manganese in the equatorial plane and the axial positions are occupied by monodentate water/py/2-pic/3-pic/4-pic molecules in complexes **1**-**5**, while in complexes **6** and **7**, the nitrogens from azomethine and bidentate bpy or phen are in equatorial positions and the naphtholate oxygens are present in axial positions. The enolate oxygens remain uncoordinated. The octahedral geometry around Mn(IV) ion is supported by the magnetic susceptibility, electronic and EPR data in all these complexes. The similarity in CVs of ligand and manganese(IV) complexes suggests the presence of only ligand-centered redox activity. The antibacterial investigations revealed that the metal complexes **6** and **7** are more effective against two Gram-negative bacteria (*Enterobacter aerogenes* and *Proteus vulgaris*) than the free ligand.

ACKNOWLEDGEMENTS

The authors are thankful to Prof. R.A. Lal and Dr. M. Velusamy, Department of Chemistry, North-Eastern Hill University, Shillong and Prof. V. Manivannan, Department of Chemistry, IIT Guwahati, Guwahati for the helpful discussions. Two of the authors (PS and PM) are also thankful to MHRD Govt. of India for RA offered under the TEQIP-III project.

CONFLICT OF INTEREST

The authors declare that there is no conflict of interests regarding the publication of this article.

REFERENCES

1. A. Kajal, S. Bala, S. Kamboj, N. Sharma and V. Saini, *J. Catal.*, **2013**, 893512 (2013); https://doi.org/10.1155/2013/893512
2. S. Adhikari, R.A. Lal, A. Debnath and D. Dey, *J. Chem. Pharm. Res.*, **9**, 236 (2017).
3. M.A.-N. Mohammed, *Periodica Polytechnica*, **56**, 83 (2012); https://doi.org/10.3311/pp.ch.2012-2.06
4. M.K. Singh, N.K. Kar and R.A. Lal, *J. Coord. Chem.*, **61**, 3158 (2008); https://doi.org/10.1080/00958970802010583
5. M.K. Singh, N.K. Kar and R.A. Lal, *J. Coord. Chem.*, **62**, 1677 (2009); https://doi.org/10.1080/00958970802676649
6. M.S. Refat, S.A. El-Korashy, D.N. Kumar and S.A. Ahmed, *Spectrochim. Acta A Mol. Biomol. Spectrosc.*, **70**, 898 (2008); https://doi.org/10.1016/j.saa.2007.10.005
7. A.H. Ahmed, A.M. Hassan, H.A. Gumaa, B.H. Mohamed and A.M. Eraky, *J. Chil. Chem. Soc.*, **63**, 4180 (2018); https://doi.org/10.4067/S0717-97072018000404180
8. R.A. Lal, A. Kumar and M.L. Pal, *J. Indian Chem. Soc.*, **76**, 70 (1999).
9. X.-H. Lu, Q.-H. Xia, H.-J. Zhan, H.-X. Yuan, C.-P. Ye, K.-X. Su and G. Xu, *J. Mol. Catal. Chem.*, **250**, 62 (2006); https://doi.org/10.1016/j.molcata.2006.01.055
10. R.O. Costa, S.S. Ferreira, C.A. Pereira, J.R. Harmer, C.J. Noble, G. Schenk, R.W.A Franco, J.A.L.C Resende, P. Comba, A.E. Roberts, C. Fernandes and A. Horn Jr., *Front. Chem.*, **6**, 491 (2018); https://doi.org/10.3389/fchem.2018.00491
11. S.-B. Yu, S.J. Lippard, I. Shweky and A. Bino, *Inorg. Chem.*, **31**, 3502 (1992); https://doi.org/10.1021/ic00043a004
12. M. Zlatar, M. Gruden, O.Y. Vassilyeva, E.A. Buvaylo, A.N. Ponomarev, S.A. Zvyagin, J.J. Wosnitza, J. Krzystek, P. Garcia-Fernandez and C. Duboc, *Inorg. Chem.*, **55**, 1192 (2016); https://doi.org/10.1021/acs.inorgchem.5b02368
13. R.A. Lal, D. Basumatary, O.B. Chanu, A. Lemtur, M. Asthana, A. Kumar and A.K. De, *J. Coord. Chem.*, **64**, 300 (2011); https://doi.org/10.1080/00958972.2010.542238
14. N.K. Chaudhary and P. Mishra, *Bioinorg. Chem. Appl.*, **2017**, 6927675 (2017); https://doi.org/10.1155/2017/6927675
15. A.I. Vogel, A Textbook of Quantitative Inorganic Analysis including Elementary Instrumentation Analysis, Longmans: London, Eds. 4 (1978).
16. W.J. Geary, *Coord. Chem. Rev.*, **7**, 81 (1971); https://doi.org/10.1016/S0010-8545(00)80009-0
17. D. Sadhukhan, A. Ray, G. Pilet, G.M. Rosair, E. Garribba, A. Nonat, L.J. Charbonnière and S. Mitra, *Bull. Chem. Soc. Jpn.*, **84**, 764 (2011); https://doi.org/10.1246/bcsj.20110004
18. H. Temel and M. Sekerci, *Synth. React. Inorg. Met.-Org. Chem.*, **31**, 849 (2001); https://doi.org/10.1081/SIM-100104855
19. N. Nishat, T. Ahamad, S. Ahmad and S. Parveen, *J. Coord. Chem.*, **64**, 2639 (2011); https://doi.org/10.1080/00958972.2011.570754
20. L. Sacconi, A. Sabatini and P. Gans, *Inorg. Chem.*, **3**, 1772 (1964); https://doi.org/10.1021/ic50022a026
21. C.W. Frank and L.B. Rogers, *Inorg. Chem.*, **5**, 615 (1966); https://doi.org/10.1021/ic50038a026
22. G. Sartori, C. Furlani and A. Damiani, *J. Inorg. Nucl. Chem.*, **8**, 119 (1958); https://doi.org/10.1016/0022-1902(58)80172-4
23. A.M. Hassan, A.H. Ahmed, H.A. Gumaa, B.H. Mohamed and A.M. Eraky, *J. Chem. Pharm. Res.*, **7**, 91 (2015).
24. M. Tyagi, S. Chandra and P. Tyagi, *Spectrochim. Acta A Mol. Biomol. Spectrosc.*, **117**, 1 (2014); https://doi.org/10.1016/j.saa.2013.07.074
25. B. Murukan and K. Mohanan, *Transition Met. Chem.*, **31**, 441 (2006); https://doi.org/10.1007/s11243-006-0011-7
26. R. Mukhopadhyay, S. Bhattacharjee, C.K. Pal, S. Karmakar and R. Bhattacharyya, *J. Chem. Soc., Dalton Trans.*, 2267 (1997); https://doi.org/10.1039/a700855d
27. J.R. Hartman, B.M. Foxman and S.R. Cooper, *Inorg. Chem.*, **23**, 1381 (1984); https://doi.org/10.1021/ic00178a017
28. H. Okawa, M. Nakamura and S. Kida, *Bull. Chem. Soc. Jpn.*, **55**, 466 (1982); https://doi.org/10.1246/bcsj.55.466
29. C.P. Pradeep, P.S. Zacharias and S.K. Das, *J. Chem. Sci.*, **118**, 311 (2006); https://doi.org/10.1007/BF02708524
30. P.J. Chirik and K. Wieghardt, *Science*, **327**, 794 (2010); https://doi.org/10.1126/science.1183281
31. M.D. Ward and J.A. McCleverty, *J. Chem. Soc., Dalton Trans.*, **3**, 275 (2002); https://doi.org/10.1039/b110131p
32. R.S. Joseyphus and M.S. Nair, *J. Coord. Chem.*, **62**, 319 (2009); https://doi.org/10.1080/00958970802236048
33. S.B. Bakare, *Pol. J. Chem. Technol.*, **21**, 26 (2019); https://doi.org/10.2478/pjct-2019-0026
34. S.M. Abdallah, M.A. Zayed and G.G. Mohamed, *Arabian. J. Chem.*, **3**, 103 (2010); https://doi.org/10.1016/j.arabjc.2010.02.006